BJP

Bangladesh Journal of Pharmacology

Research Article

The Role of Cell Wall Mutation in the Pathogenicity of E. coli H7:O157: A Molecular Evolution Study

A Journal of the Bangladesh Pharmacological Society (BDPS)
Journal homepage: www.bdpsjournal.org; www.banglajol.info
Abstracted/indexed in Academic Search Complete, Agroforestry Abstracts, Asia Journals Online, Bangladesh Journals Online, Biological Abstracts, BIOSIS Previews, CAB Abstracts, Current Abstracts, Directory of Open Access Journals, EMBASE/Excerpta Medica, Global Health, Google Scholar, HINARI (WHO), International Pharmaceutical Abstracts, Open J-gate, Science Citation Index Expanded, SCOPUS and Social Sciences Citation Index
Bangladesh J Pharmacol 2026; 21: 8-21
ISSN: 1991-0088

The Role of Cell Wall Mutation in the Pathogenicity of E. coli H7:O157: A Molecular Evolution Study

Walaa A. Salloomi[1], Rebah N. Algafari[2]*, Ikram Abbas Abbood[1]

[1]Department of Microbiology, College of Veterinary Medicine, Baghdad University,

*[2]*Depart-ment of Environmental Biotechnology, Biotechnology Research Center, Al-Nahrain Uni-versity*

[3]Department of Microbiology, College of Veterinary Medicine, Baghdad University,.

**Correspondening Author*

Rebah N. Algafari

Article Info

Cite this article:
Walaa A. Salloomi, Rebah N. Algafari, Ikram Abbas Abbood. The Role of Cell Wall Mutation in the Pathogenicity of E. coli H7:O157: A Molecular Evolution Study. Bangladesh J Pharmacol. 2026; 21: 8-21.

Key words E. coli H7:O157; microbial pathogenesis; bacterial cell wall modification; site-directed mutagenesis

Abstract

E. coli H7:O157, the cauWallsative pathogen of many disease outbreaks and food poisoning cases, is the subject of many studies. The bacterium's pathogenicity is highly associated with cell wall modi-fications and changes. A total of 20 fecal samples from patients who showed typical symptoms of the infection and tested positive for E. coli H7:O157 were collected. Another 20 samples from ani-mals that showed signs of infection with this bacterium were also collected and processed. The bac-terium was isolated and identified using cultural and molecular methods. The waa K, waa L, and waa Y sites were subjected to site-directed mutagenesis, and the effect of these mutations was studied and analyzed through their influence on the pathogenicity compared to the wild type. We found that the invasiveness and morbidity of mutant E. coli H7:O157 increased significantly when ingest-ed by laboratory animals. This may be attributed to waa K and waa L since they led to a significant change in the transmembrane helix ratio compared to the wild type, enabling the uncontrolled re-lease of the Shiga toxin into the infected animals and causing their death in 6 h. Specific sites in the waa operon, namely waa K and waa L, play the leading role in controlling the progress of patho-genicity. Mutations in these sites may increase the virulence of this bacterium.

Introduction

The Shiga toxin-producing *E. coli* O157:H7 (STEC) was identified in 1982 as a human pathogen [1]. *E. coli* O157:H7 was thus named due to its ability to express the somatic (O) antigen with the flagellar antigen (H) [2]. MacConkey agar supplemented with MUG and sorbitol was used to identify and select the original isolate of *E. coli* O157:H7 [3]. STEC is a zoonotic pathogen causing worldwide outbreaks [2] with the virulence factors Shiga toxins 1 and 2 [4]. Additional virulence factors have been identified, represented by plasmid-encoded enterohemolysin (EhxaA), autoagglutination adhesion (Saa), and catalase-peroxidase (KatP) [5]. This strain is also known as enterohemorrhagic *E. coli* (EHEC) and can cause hemorrhagic colitis (HC), which can be life-threatening, with sequelae including hemolytic uremic syndrome (HUS) [6]. The bacterium has also been isolated from animals (farm livestock). The spread of such an infection may lead to a decline in animal production, especially in the case of poultry and large animals, due to abdominal sepsis, urinary tract infections, blood poisoning, and diarrhea [7].

E. coli O157:H7 is transmitted through food, such as dairy products and vegetables contaminated with the feces of infected animals [7,8]. Large animals like sheep and cattle are the fundamental reservoirs of *E. coli* O157:H7 [9,10]. Pets like birds and dogs can be considered a secondary route of infection [11].

Intestinal colonization by *E. coli* O157:H7 is accompanied by damage to lining cells due to the production of Shiga toxin [12]. The bacterium can resist the host's defense mechanism and mimics part of the normal intestinal flora [13]. Adhesion to intestinal epithelial cells is considered the first step in STEC interactions, and the binding patterns of STEC and epithelial cells are unique to *eae*-negative STEC strains [14]. Many EHEC strains are *eae*-positive, and the *eae* gene is considered a risk factor for HUS [15].

The genome size of *E. coli* O157:H7 is 5.5 Mb, with a 4.1 Mb backbone sequence conserved in *E. coli* strains [16]. When the genome size of *E. coli* O157:H7 was compared with that of non-pathogenic *E. coli*, about 0.53 Mb was missing in the former, suggesting that an evolutionary mechanism played a role in the

development of this strain [17,18].

Antibiotic resistance is one of the characteristics of *E. coli* O157:H7 that increases its pathogenicity. It has been found to be highly resistant to quinolones, aminoglycosides, macrolides, and others [19]. In addition to the occurrence of *E. coli* O157:H7, the spread of other antimicrobial-resistant bacteria and multidrug-resistant zoonotic foodborne pathogens has become a worldwide problem [20]. Resistance genes are the main cause of antibiotic resistance, but the cell wall and the shape transition of the cell may also play critical roles in this mechanism [21, 22]. Some studies [23,24] have addressed chemical modifications, the destruction of antibiotics, or changes in the cell wall structure that inhibit antibiotic action, but the molecular underpinnings of such changes need to be addressed and clarified. Thus, this study aimed to determine the tendency of the bacterium cell mutation, the consequence of this mutation on the bacterium, and its effect on the pathogencity and ability to infect the target host.

Recent studies concerning *E. coli* isolated from certain populations and its antimicrobial resistance (AMR) indicated that the profile of this criterion is correlated with the same species isolated from sewage samples. This means *E. coli* can be an important indicator to evaluate the impact of human activity on the environment, wild animals, and aquatic animals with a high risk of acquiring AMR [25].

Materials and Methods

2.1. Ethics and Participation in This Study

Animal Welfare and IRB Approval

The Biotechnology Research Center's IRB at Al-Nahrain University issued ethical approval for experiments potentially impacting animal welfare with reference no. PG/244, following EU Directive 2010/63/EU.

Human Sample Collection Approval

The Biotechnology Research Center at Al-Nahrain University approved human sample collection after patients provided written consent—an ethical approval document with the reference no. C.B 242 was issued for this purpose.

Sample Collection

A total of 40 fecal samples and watery intestinal exudates released by human patients admitted to Al-Yarmouk Teaching Hospital or Al-Kindy Teaching Hospital were collected. The samples were immediately processed at the clinical laboratories of the hospitals by cultivation in nutrient broth and then transferred to the university's laboratories for further processing after 24 h.

Furthermore, 40 animal feces samples were collected from Al-Ridhwanyia, Abu Gharib, and Al-Dora farms from large animals, such as cows and sheep, showing symptoms of diarrhea, cold extremities, unsteadiness, and difficulty standing. The samples were preserved in a transport medium and transferred to the university's laboratories using a cool box. Upon arrival, these samples were diluted with sterile normal saline and cultured in nutrient broth for 24 h to enable bacterial growth.

Isolation of *E. coli* O157:H7

Samples enriched in nutrient broth were diluted to 10^6 and cultivated on MacConkey agar (Oxoid, London, UK) for 24 h at 37 °C. Colorless colonies were transferred and spread on Eosin Methylene Blue agar (EMB) (Hi Media, New Delhi, India) and allowed to grow for 24 h at 37 °C. *E. coli* colonies that showed a metallic sheen were selected and cultivated on Hi Chrome medium with supplements (Hi Media, New Delhi, India) for 24 h at 37 °C. Colonies of *E. coli* O157:H7 exhibited a dark purple to magenta color.

Molecular Identification of E. coli O157:H7

Extraction of DNA from Bacterial Cells

DNA was extracted from the cultivated colonies obtained from sample culturing using the GenX total DNA extraction kit (Yorkshire, UK) according to the manufacturer's instructions. About 105 µg of DNA was obtained on average from each bacterial sample, with a purity of 1.8, as measured by the NanoDrop system (Techne, London, UK). DNA samples were preserved at −20 °C until processing.

PCR Amplification of Specific *E. coli* O157:H7 Genes

E. coli O157:H7 possesses a unique set of genes by which it can be easily identified. The following genes were detected in the isolate under study.

Specific primers were used to amplify the *rpo*B gene, with the gene sequence deposited within the NCBI database under accession no. JX471606. The sequences of the primers are rpF 5′ CAGCCAGCTGTCTCAGTTTAT 3′ and rpR 5′ GGCAAGTTACCAGGTCTTCTAC 3′. The thermocycler (LabNet, Massachusetts, USA) program involved one cycle of denaturation at 95 °C for 2 min, followed by 35 cycles of denaturation at 94 °C for 30 s, annealing at 49 °C for 30 s, and extension at 72 °C for 30 s. The samples were then subjected to a final extension at 72 °C for 10 min and held at 4 °C until they were removed from the thermocycler. The obtained amplicons were preserved at −20 °C.

. The *waa* gene amplification primers

This site was amplified with specific primers based on the gene sequence with accession no. M95398 in the NCBI database. The primer sequences were as follows: waa F 5′ CACTAATTTTACGTGGCAGAC 3′ and waa R 5′ CCCATATGATCACATCAACTGA 3′. The thermocycler program involved one cycle of denaturation at 95 °C for 2 min, followed by 35 cycles of denaturation at 94 °C for 30 s, annealing at 59 °C for 30 s, and extension at 72 °C for 30 s. When the samples were completely amplified, they were subjected to a final extension at 72 °C for 10 min and held at 4 °C.

The Shiga Toxin *stx* gene amplification primers

The following primers were designed to amplify *the stx* 1 gene based on the accession number OM304351 in the NCBI database. The primer sequences were stxF 5′ CAGTTAATGTCGTGGCGAAGG 3′ and stxR 5′ CACCAGACAATGTAACCGCTG 3′. The gene was amplified using the following program: 95 °C (1 cycle), denaturation at 94 °C for 30 s, annealing at 55 °C, and extension at 72 °C (35 cycles). Final extension was conducted at 72 °C for 10 min, and the samples were held at 4 °C.

The *rfb*O gene amplification primers

The *rfb*O was targeted for amplification by PCR using specific primers based on accession no. X59852 from the NCBI. The primers' sequences were rfoF 5′ CGTGATGATGTTGAGTTG 3′ and rfoR 5′ AGATTGGTTGGCATTACTG 3′. PCR

amplification of the target gene was performed under the following conditions: one cycle of initial denaturation at 95 °C for 2 min, followed by 35 cycles of denaturation at 94 °C for 30 s, annealing at 59 °C for 30 s, and extension at 72 °C for 30 s. The final extension was performed at 72 °C for 10 min, and the samples were held at 4 °C until they were removed from the thermocycler.

A primer was used for site-directed mutagenesis and the cloning experiment.

The cell wall-controlling operon *waa* was targeted for mutagenesis. A primer was designed using the software available at https://nebasechanger.neb.com accessed on 11.5.2023. The primer used for site-directed mutagenesis, after adding the sticky ends complementary to the cloning vector, is highlighted in gray. The primer sequences were mutCF 5′ T CAG CAA GGG CTG AGGcgcacatcctttaaacttcattcattg 3′ and mutCR 5′ catttaattaattgtattgttacgattattaatgG GGA GTC GAA GGC GACT 3′. The PCR program involved initial denaturation at 95 °C for 2 min (1 cycle), followed by 30 cycles of denaturation at 94 °C, annealing at 63 °C for 1 min, and extension at 72 °C for 1 min. The final extension was performed at 72 °C for 10 min, and the samples were held at 4 °C after the reaction was completed.

Site-Directed Mutagenesis

The PCR product of the *waa* gene was used as a template for the mutagenesis experiment. An amount of 2 µL of PCR *waa* amplicon was mixed with 1 µL of mutCF and 1 µL of mutCR (the final concentration was 0.5 pmol of each primer) in a master mix tube (Bioneer, Korea) and subjected to PCR amplification according to the following program: initial denaturation at 95 °C for 2 min (1 cycle), followed by 30 cycles of denaturation at 94 °C, annealing at 62 °C for 1 min, and extension at 72 °C for 1 min. The final extension was performed at 72 °C for 10 min, and the samples were held at 4 °C after the reaction was completed.

Cloning of the Mutated *waa* Gene

Cloning of the mutated *waa* gene was performed using the MB324 NZYEasy Cloning & Expression kit (NZYTech, Lisbon, Portugal).

Transformation Procedure

The transformation procedure was performed for both competent cells (NZYTech DL3 star *E. coli*) and the wild type. The transformation protocol was achieved with the following steps: A volume of 10 µL of ligation product obtained from the cloning experiment was mixed directly with 100 µL of recipient cells and placed on ice for 30 min. The mixture was removed and subjected to heat shock at 42 °C for 40 s and placed on ice again for 2 min. A pre-warmed SOC medium was added to the cells and incubated at 200 rpm at 37 °C for 1 h. The cells were then precipitated by centrifugation at 5000 rpm for 1 min, and the remaining medium was removed. After precipitation, the cells were gently re-suspended by pipetting, and 100 µL of the cells were spread on LB agar plates with 50 µg/mL kanamycin. The plates were incubated at 37 °C overnight to allow only the transformant to grow.

The same protocol was used to transform wild-type *E. coli* with one modification, which involved treating the cells with lysozyme (10 µg/mL) for 1 h at 4 °C before proceeding to the transformation protocol.

Confirmation of Cloning and Transformation

The mutated gene was cloned and transformed to the recipient bacterium and confirmed by electrophoresis. An amount of 2 µL of standard mixture pHTP9 (provided by the manufacturer company) with sequences pHF 5′ GAATGAAAAACGCGACCACATGGTG 3′ and pHR 5′ GGTTATGCTAGTTATTGCTCAGCG 3′ and primers mutCF, and mutCR were mixed and used to amplify the mutated gene, and the transformation was confirmed by pHTP9. The difference in DNA bands (one band from the colony with a cloning vector only and two bands from the colony with a mutated gene) was resolved by electrophoresis, which differentiates between the standard cloning product and the one with a mutated gene. Colony PCR was performed to confirm successful cloning and transformation.

Sequencing of PCR Products

PCR products were sent to Macrogen Corp. (Korea) for sequencing using the Sanger method.

Animal Experiment

The experiment was performed with 180 BALB/c mice, which were divided into 3 groups. Each group contained 60 mice that were further subdivided into groups of 30, except for the third group containing the control mice, resulting in a total of five groups named and treated as follows: group 1-1 was infected with wild-type *E. coli* O157:H7 without treatment; group 1-2 was infected with wild-type *E. coli* O157:H7 and treated with cefotaxime; group 2-1 was infected with mutated *E. coli* O157:H7 and left without treatment; and group 2-2 was infected with mutated *E. coli* O157:H7 and treated with cefotaxime. The third group, comprising the control mice, was kept away from the other groups to prevent infection with the pathogen. Blood was drawn from groups 1 and 2 when they showed symptoms of infection, as identified by a professional veterinarian, and both liver and kidney function were measured for comparison with mice in the same group and other groups.

Data Analysis and Bioinformatics

Sequences obtained by PCR amplification were analyzed using tools available on the NCBI website (https://www.ncbi.nlm.nih.gov). We used BankIt (accessed on 20.7.2023) to confirm the results of the DNA sequence obtained from PCR amplification and to deposit the DNA sequence of different genes identified during the study (https://submit.ncbi.nlm.nih.gov/about/bankit/). The BLAST (version 2.17.0 accessed on 20.7.2023) of the DNA sequences was carried out using the BLASTN tool (https://blast.ncbi.nlm.nih.gov/Blast.cgi?PROGRAM=blastn&PAGE_TYPE=BlastSearch&LINK_LOC=blasthome), amino acid residues were identified through BLASTX (https://blast.ncbi.nlm.nih.gov/Blast.cgi?PROGRAM=blastx&PAGE_TYPE=BlastSearch&LINK_LOC=blasthome), and Phyre2 (version 2.2 accessed on 15.8.2023) was used to build the secondary and tertiary structures of encoded proteins http://www.sbg.bio.ic.ac.uk/phyre2/html/page.cgi?id=index.

Statistical Analysis

The Statistical Packages of Social Sciences (SPSS 2018) was used for statistical analysis. The parameters measured during the study were input to calculate the least significant difference (LSD) to evaluate the statistical significance of the differences among the tested groups.

Results

3.1. Isolation of E. coli O157:H7 and Morphological

Characteristics

Among all of the samples obtained from humans and animals, only 20 from each group were positive for *E. coli*. The isolation and identification of the bacterium were performed using culture media before molecular methods. Colonies with a mauve color, which is a characteristic of *E. coli* O157:H7, were selected for further study. Figure S1 in the Supplementary Materials shows the growth of *E. coli* O157:H7 on different media.

Molecular Identification and Classification of E. coli O157:H7

The *rpoB* gene was amplified and sequenced, and the BLAST was used to identify and classify the bacterium under study. The results of PCR amplicon sequencing show that it belongs to the *E. coli* O157:H7 strain Sakai, and our sequence was deposited in the NCBI database under accession no. PP059841. Figure S2 shows the electrophoresis results of the *rpoB* gene amplified from isolates from humans and animals (Supplementary Materials).

The waa Gene

The *waa* gene was amplified by PCR using specific primers designed for this purpose, and the resulting amplicons were sequenced and analyzed. The results show that the gene belongs to the *E. coli* O157:H7 strain Sakai, and it was deposited in the NCBI database under accession no. PP059843. Figure S3 (Supplementary Materials) shows the electrophoresis of the *waa* gene obtained by PCR amplification.

The Shiga Toxin Gene stx

Production of Shiga toxin is one of the main characteristics of *E. coli* O157:H7. Our initial survey showed that it is a type 1 Shiga toxin, and it was amplified by PCR and analyzed. The obtained sequence was deposited in the NCBI database under accession no. OR939814. Figure S4 shows the electrophoresis of the amplified *stx1* gene (Supplementary Materials).

The rfbO Gene

The *rfbO* gene is characteristic of *E. coli* O157:H7. It encodes the O antigen, which is a major component of the bacterium's cell wall. During this study, this gene was targeted for amplification and sequencing and was found to be similar to the *E. coli* O157:H7 strain Sakai. The sequencing results were deposited in the NCBI database under accession no. PP059842. Electrophoresis of the amplified *rfb*O gene is shown in Figure S5 (Supplementary Materials).

Site-Directed Mutagenesis of the waa Gene

The *waa* gene was obtained by PCR amplification and subjected to mutagenesis using a primer specifically designed for this purpose. This primer targeted the sequences on the gene responsible for protein coding, resulting in mutated gene products that encode mutated proteins predicted to be incorporated into the cell wall. The verification of the site-directed mutagenesis of the *waa* gene is shown in Figure 1.

Cloning and Transformation of the Mutated waa Gene

The mutated *waa* gene was cloned into the pHTP9 cloning vector. The product of the cloning experiment was used to transform competent cells and wild-type strains. Positive selection was the basis on which the transformants were selected since they can resist kanamycin due to the resistant gene harbored by pHTP9. When transformants could grow on LB agar supplemented with kanamycin, we performed colony PCR using primers mutC and pH to target the mutated gene and a specific sequence on pHTP9, respectively. This confirmed that the transformation procedures were successful. Figure S6 (Supplementary Materials) shows the growth of transformants on kanamycin-supplemented LB medium compared to normal cells, whereas Figure 2 shows the result of the colony PCR.

Interpretation of Site-Directed Mutagenesis of the waa Gene

Mutated *waa* K

The *waa* K gene is responsible for n-acylglucoseamine transferase synthesis, and its product is involved in the modification of the LPS core before attachment to the O antigen. This site was targeted for mutation to investigate the effect of the newly encoded protein on the bacterium. The results are shown in Table S1 (Supplementary Materials).

The *waa* L Gene

The *waa L* gene product is involved in core modification and O antigen coding. A mutation in this gene requires the specific criteria shown in Table S2 (Supplementary Materials).

The *waa* Y Gene

The *waa Y* gene's role is to modify the cell, which increases the size of the LPS. Mutation of this gene was performed to study specific characteristics that may be important to cell wall formation. Table S3 (Supplementary materials) shows the changes in this gene's characteristics.

Cell Wall Topology of Mutated *E. coli* Compared to the Wild Type

In all kinds of bacteria, the cell wall is characterized by a specific topology that enables chemical and biochemical compound exchange and allows for efficient interaction with the environment. Changing the protein structure of the cell wall may cause its topology to change. The topologies of the cell walls of wild-type *E. coli* and the mutated type were determined in our experiment and summarized in Table 1.

Moreover, the transmembrane topologies in both types of bacteria were significantly changed. This can be seen through the arrangement of the spanning proteins integrated in the cell wall and illustrated in Figure 3.

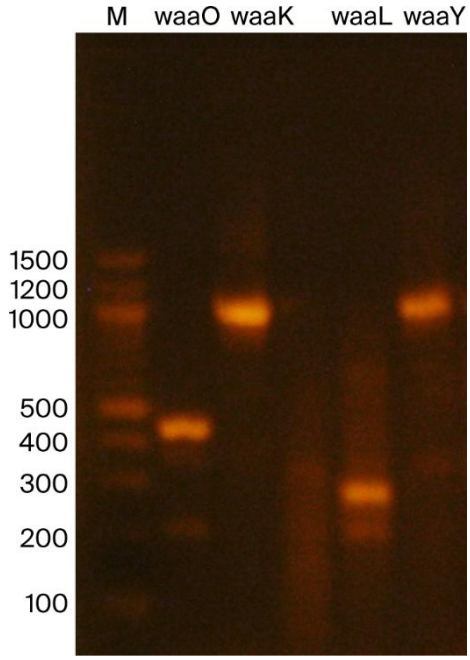

Figure 1. Electrophoresis of the mutated *waa gene* amplified from *E. coli* O157:H7. M is a 100 bp marker DNA. Lanes 1, 2, and 3 represent the mutated *waa* gene.

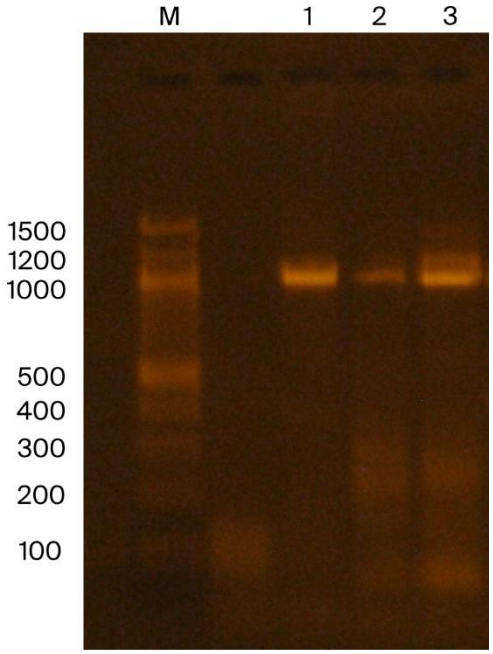

Figure 2. PCR amplification of the mutated gene and pHTP9. M1 is a 500 bp DNA marker, and M2 is a 100 bp DNA marker. Lane 1 shows the amplification results of pHTP9, lane 2 shows the amplification results of the mutated gene, and lane 3 shows the amplification results of pHTP9 carrying the mutated gene.

Table 1. Topology and characteristics of mutated *E. coli* compared to the wild type.

The 3D Structure of Mutated *waa* Gene	Expected Biological Function
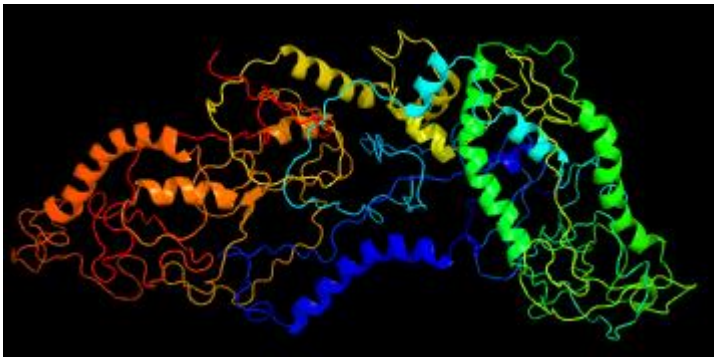 image colored by rainbow N → C terminus Model dimensions (Å): X:111.214 Y:67.138 Z:102.658	Putative membrane antigen

Secondary structure of mutated *waa* gene

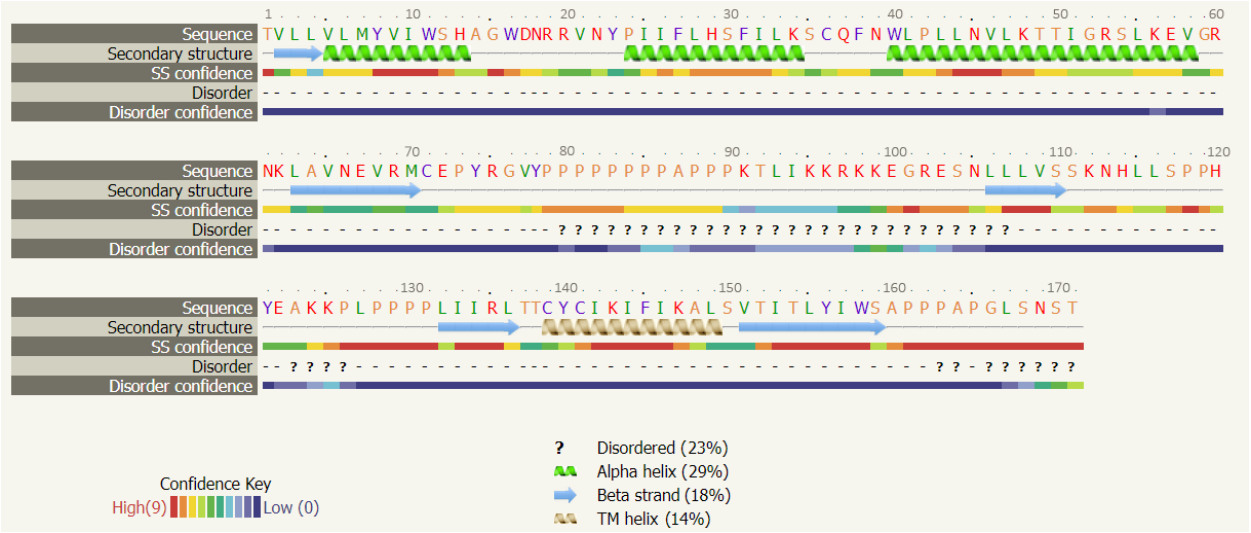

Function conservation of mutated *waa* gene	Conserve amino acid residues in mutated protein	Position in the sequence
	Uncharacterized	
Mutational sensitivity of mutated *waa* gene	Highly sensitive amino acid residues in mutated protein	Position in the sequence
	Uncharacterized	
The 3D structure of wild-type cell wall		Expected biological function

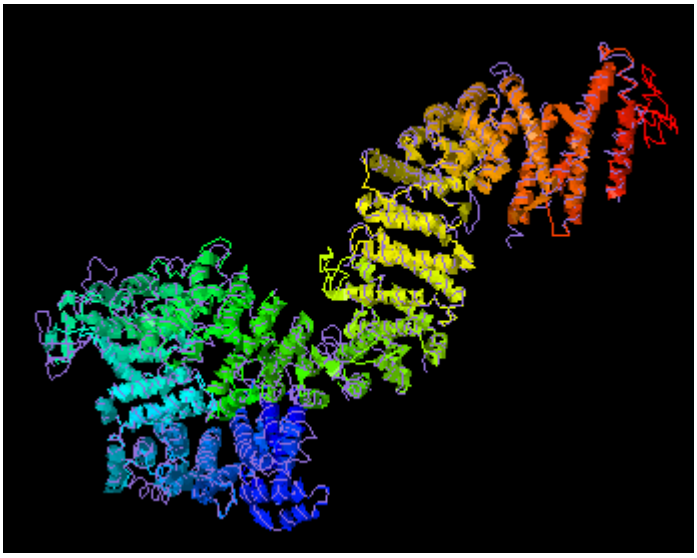

Single-particle Cryo-EM Structure of the *waa* L O-antigen ligase in its ligand bound state, lipopolysaccharide heptosyltransferase-1

image colored by rainbow N → C terminus
Model dimensions (Å): X:47.053 Y:64.719 Z:48.441

Secondary structure of wild-type *waa* gene

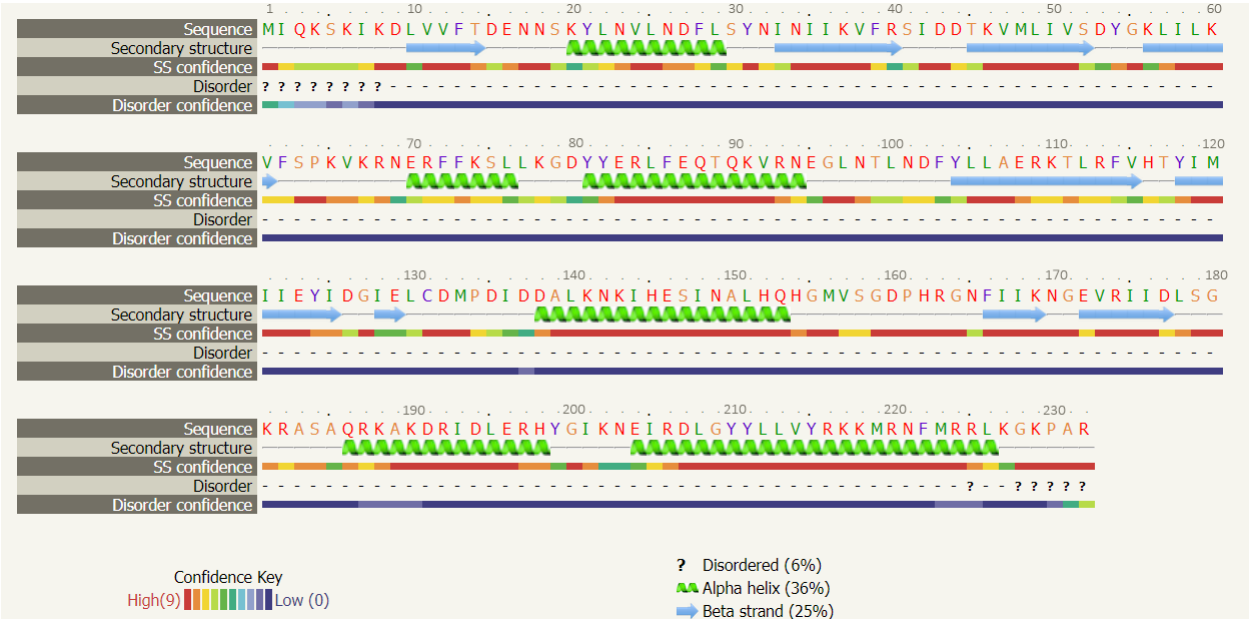

Function conservation of wild-type *waa* gene

Conserve amino acid residues in wild-type protein

Position in the sequence

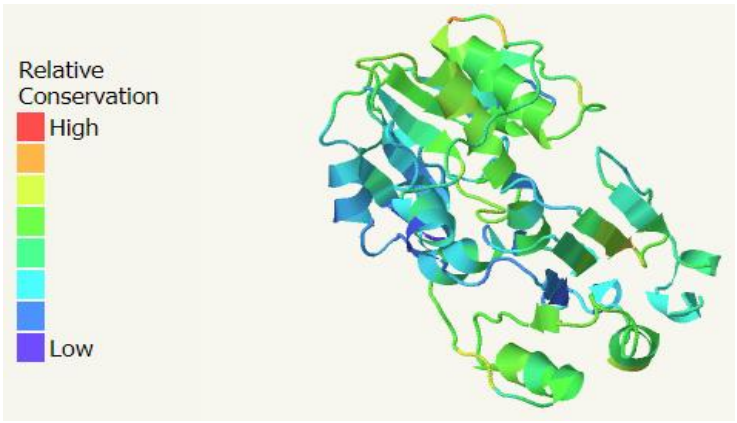	W, Y, Y, Y, P, R, R, Y, P, H, N, Y, H, D, F, D, H, W, E, A, D, P, Y, N, E, Y, Y	88, 106, 137, 152, 218, 265, 288, 292, 303, 380, 239, 368, 466, 529, 565, 706, 711, 737, 889, 951, 970, 999, 1013, 1015, 1039, 1050, 1057
Mutational sensitivity of mutated *waa* gene	Highly sensitive amino acid residues in mutated protein	Position in the sequence
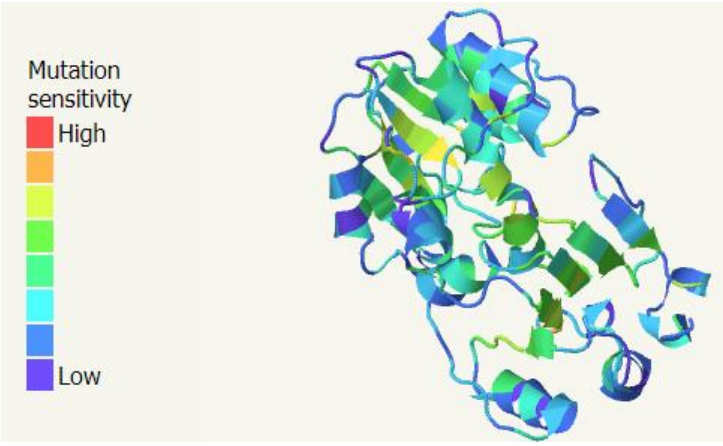	H, W, Y, R, Q, P, R, G, R, Y, P, H, H, N, G, G, K, D, P	9, 88, 152, 161, 115, 118, 165, 186, 288, 292, 303, 336, 338, 339, 349, 352, 539, 634

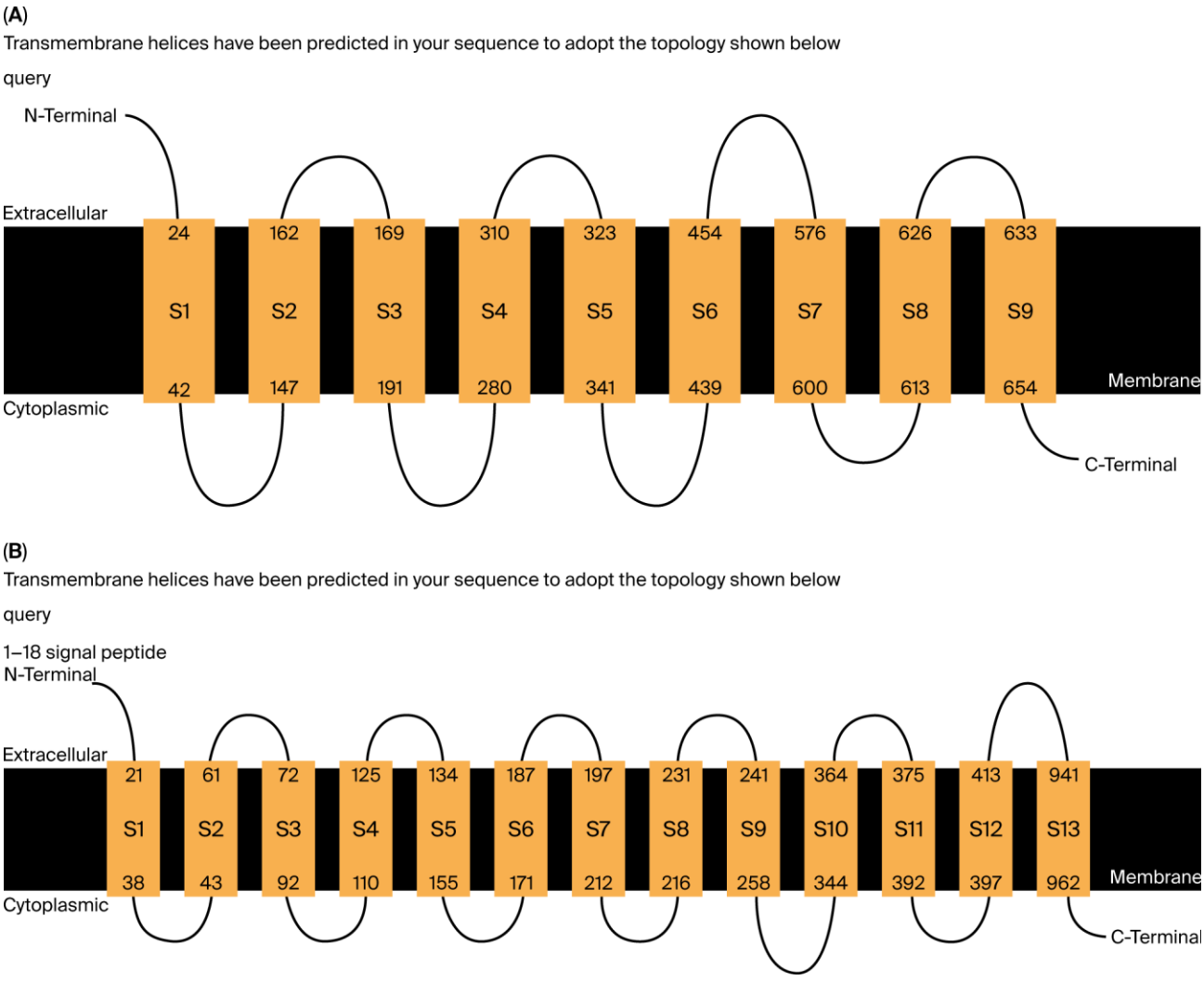

Figure 3. The arrangement of the transmembrane of mutant *E. coli* H7:O157 (**A**) and wild-type *E. coli* H7:O157 (**B**). The figure shows a significant change in the spanning proteins in the cell wall.

Table 8. Changes in type and location of amino acid residues in the mutated and wild-type cell walls of *E. coli* H7:O157.

Mutated Cell Wall (733 Residues)			**Wild-Type Cell Wall (1453 Residues)**		
Location on the cell wall	A.A. sequence	Type of helix	Location of A. A. residue	A.A. sequence	Type of helix
Outside	1–19	α/β	Inside	1–19	α/β
	20–42	TMhelix		20–37	TMhelix
Inside	43–144	α/β	Outside	38–40	α/β
	145–162	TMhelix		41–60	TMhelix
Outside	163–166	α/β	Inside	61–71	α/β
	167–186	TMhelix		72–91	TMhelix
Inside	187–290	α/β	Outside	92–105	α/β
	291–310	TMhelix		106–128	TMhelix
Outside	311–319	α/β	Inside	129–134	α/β
Inside	320–436	α/β		135–157	TMhelix
	437–459	TMhelix	Outside	158–166	α/β

Outside	460–733	α/β		167–189	TMhelix
			Inside	190–195	α/β
				196–213	TMhelix
			Outside	214–239	α/β
				240–259	TMhelix
			Inside	260–345	α/β
				346–368	TMhelix
			Outside	369–371	α/β
				372–394	TMhelix
			Inside	395–398	α/β
				399–418	TMhelix
			Outside	419–1453	α/β

When applying the Hidden Markov Model (HMM) to both cell walls, significant changes were also predicted and are listed in Table S6 (Supplementary Materials).

In the types of cell walls studied and predicted, the distribution of both α/β and TM helices was significantly changed regarding their location and the A. A. residues involved in this change, as illustrated in Table 8. 3.9. Laboratory Animal Experiment and Statistical Analysis

Measuring Liver Function in Infected Animals

Wild- and mutated-type *E. coli* O157:H7 were orally administered to the experimental animals. The animals were observed for infection symptoms, and blood was drawn from all animals that showed signs of weakness, diarrhea, and disturbed or weak motion. The liver function of the tested animals was measured and compared, as shown in Table S4 (Supplementary Materials).

Measuring Kidney Function

Infection with *E. coli* O157:H7 can disturb an animal's physiological functioning. Among the indicators of infection is the disturbance of kidney function, represented by elevated blood urea and serum creatinine. Measurements of these factors are given in Table S5 (Supplementary Materials).

Discussion

Diseases causing diarrhea are considered to be a serious threat to health and well-being. Among these diseases are those caused by *E. coli* [25,26]. *E. coli* O157:H7 can be identified using emerging high-throughput methods, such as isothermal DNA amplification, surface-enhanced spectroscopy, biosensors, and rapid paper-based diagnostic methods [27,28].

The lipopolysaccharide (LPS) is the main component of the outer membrane of Gram-negative bacteria, including *E. coli*. It is composed of lipid A, an oligosaccharide core made of glucose, heptose, galactose, 2-keto-3-deoxyoctonate (KDO), and a highly variable component of the O antigen. The location on the chromosome responsible for LPS synthesis is called *waa* and is composed of three operons. Mutations in *waa* may lead to a truncated LPS with pleotropic effects for bacterial cells, resembling sensitivity to antibiotics and susceptibility to bacteriophages [29]. Therefore, studying mutations of the *E. coli* O157:H7 cell wall may provide crucial information about the pathogenicity, infectivity, and severity of symptoms. The Waa K product is responsible for encoding *N*-acetylglucosamine transferase and participates in the surface O antigen by facilitating the *N*-acetylglucosamine matrix, but it is not absolutely necessary for this purpose [30]. In our study, the wild-type Waa K product was identified as UDP-glycosyltransferase/glycogen phosphorylase, which is the normal function of this location in *the waa* cluster, while in the mutated type, it was identified as a transcription factor, indicating the loss of its identity. Through analysis of this gene, the protein showed an alpha helix change from 36% in the wild type to 27% in the mutant and a beta helix change from 13% to 22%. Interestingly, the loss of the transmembrane helix in the mutated gene was measured at 4% in the wild strain.

The function of the mutated gene was totally diminished compared with the wild type, which showed a tendency to lose its function at residues distributed along the gene's DNA sequence. Moreover, the mutational potential in this site seems to be high when tested under the Markov model, starting from amino acid residue 1 and ending with 120, with short intervals between them (Table 1). In an earlier study [31], the function of *waa* K seemed to be the addition of the α-1,2 terminal to *N*-acetylglucosamine, which forms a branched residue in the outer membrane. Even with a mutated *waa* K, the *N*-acetylglucosamine still has α-1, 2-linked Glc residue at the same position [32]. Thus, it seems that a mutation in this *waa* location does not have high significance regarding the cell structure or other biological functions but acts only as a complement to *the waa* L gene [33]. The *waa* L gene is the only gene known to be required for O antigen ligation during bacterial cell formation [34]. Although considerable information regarding *waa* L has been garnered from in vivo studies, researchers try to further understand the role of this gene through mutation studies [35].

In our study, the sequence was identified as a putative cell su*rfa*ce polysaccharide polymerase/ligase of the *waa* L O antigen in the wild type. After mutating this site, the original function changed to that of a beta-galactosidase enzyme. The alpha helix changed from 72% in the wild type to 23% in the mutant, and the beta helix changed from 0% in the wild type to 20% in the mutant. The significance of this mutation is that the transmembrane helix was reduced from 52% in the wild type to 12% in the mutant version of the bacterium, leading to the low function preservation represented by most amino acid residues along the encoded protein. The mutational hot spots changed when the two types of bacteria were compared (Table 2 supplementary materials).

The *waa* L mutant is unable to cap the lipid A-core with relaxed specificity for the polymer to which it attaches, and it is essential for O antigen transfer to the cell; it significantly contributes to cell wall topology [36]. Previous reports showed that if the *waa* L loses its function, it will result in a full-length

core OS that is not capped by O-PS [37]. The *waa* Y product is part of *the waa* P gene responsible for the phosphorylation activity during cell wall formation. The *waa* Y product is located in the central part of the *waa* operon and is involved in the assembly of the core region of the LPS molecule. The loss of this gene activity resulted in the loss of phosphoryl substituents [38]. In this study, we investigated the effect of mutation on the function of *waa* Y. There was a significant shift in this gene function. Instead of performing kinase activity on the heptose molecule, it shifts to transferase activity (Table S3 Supplementary Materials). This can be explained by transmembrane helices formed in the mutant type that were not detected in the wild type, which reached 14% of the secondary structure of the protein. Furthermore, both the alpha and beta helices in the wild type changed from 36% and 25% to 29% and 18%, respectively. Mutation susceptibility was found to be very low in the wild type and limited to the G, F, and H residues located at 127, 178, and 198 of the protein but increased in the mutated protein. According to our study, it seems that the *waa* Y gene is a highly preserved location due to its low susceptibility to genetic change, with the essential function of LPS phosphorylation, as previously reported [39,40].

Cell Wall Topology

This study showed that the site-directed mutagenesis inflicted on multiple essential *waa* sites may facilitate the prediction of a form of cell wall topology that *E. coli* H7:O157 can obtain. We found that, despite multiple mutations in the *waa* operon, the bacterium still keeps the O antigen characteristic on its surface, suggesting that even with the *waa* L mutation, the cell possesses an alternative mechanism to include this protein. We observed that after reconstruction of the whole surface LPS of mutated-type *E. coli* H7:O157 (Table S4 Supplementary Materials) there was a change in the secondary structure helices to form a transmembrane type, resulting in a decrease of about 14% compared to the wild type. We were unable to determine function preservation and mutational hot spots in the mutated type, while in the wild type function preservation was moderate with a low tendency for mutation, as shown in Figure 3.

Effect of Mutation on E. coli O157:H7 Infectivity and Pathogenicity

There are certain *E. coli* isolates associated with diseases in humans and animals worldwide [41] with different virulence strategies [42,43]. Studies have shown that *E. coli* pathogenicity may be attributed to the harboring of genes that resist antimicrobial agents, the formation of biofilm [44], or the production of toxins such as α-hemolysin [45] and cytotoxic necrotizing factor 1 [46]. In our experiment, laboratory animals were exposed to both wild-type and mutated *E. coli* H7:O157 to determine the effect of cell wall mutation on this bacterium's pathogenicity and morbidity. The mice exposed to the mutant *E. coli* H7:O157 showed infection symptoms within about 24 h, and half of them died within 6 h of infection symptoms appearing. When compared to the group infected with wild-type *E. coli* H7:O157, the morbidity and mortality time doubled. This can be explained by the significant release of Shiga toxin that destroyed the intestines of the mice and spread through their blood, causing significant elevations in liver and kidney enzymes, as illustrated in Tables 7 (supplementary materials) and table 8. Thus, infection with mutant *E. coli* H7:O157 caused direct hemolytic uremic syndrome (HUS) [47,48]. In normal cases of infection with EHEC, the toxin is released as a free protein liberated from the periplasmic space or enclosed in the outer membrane, ready to be released by Gram-negative bacteria [49]. In our study, the cell wall structure of the mutated bacterium is significantly changed, which might eventually lead to the uncontrolled release of the Shiga toxin into the lab animals' intestines, or it may be retained in the outer membrane until it is ready to release on demand, which is why we expected a lack of Shiga toxin cluster formation [50,51]. The *waa* operon contains other genes that may affect the pathology of the bacterium, which we could not address, representing a limitation of this study. Future studies should determine these genes' effects on antibiotic resistance and the ability of *E. coli* H7:O157 to infect their hosts.

There is an increased concern among the research society regarding antibiotic resistance [52]. Achieving balance between determining AMR bacteria and creating novel antibiotics is a challenge. If changes are not made, antibiotic resistance is expected to cause 10 million human deaths per year by 2050 [53]. Alternative strategies involve combining target-specific antimicrobial agents with multitarget drugs, with one example being metal(loid)-based antimicrobials (MBAs)/metalloantibiotics [54]. For the past several decades, silver, copper, and zinc have been increasingly used in wound dressings, drugs, and antimicrobial creams in the medical field and for odor control in textiles such as silver-containing fabrics. Current interest in metal ions and metal ion-containing molecules as antimicrobials is driven by the idea that they are a multitarget mode of antimicrobial action in contrast to most conventional antibiotics, which are predominantly single-target drugs [55].

Conclusions

E. coli H7:O157 is highly abundant in foods derived from animal products or exposed to infected animal feces and is the main cause of many outbreaks and severe infections that may be life-threatening. It is characterized by the production of Shiga toxins, which inflict damage to the small intestine, colonized by the bacterium and considered the main virulence factor. The bacterium's tendency to resist antibacterial agents is known to be a progressive trait and represents another virulence factor. The main control system in these cases is the cell wall, through which material exchange takes place. When the cell is subjected to change, the bacterium becomes more aggressive, and the production of Shiga toxins increases dramatically. Our investigation showed the modification of the cell wall topology, which occurred on a molecular level when one or more genes within the *waa* operon were changed. *waa* L and *waa* K were found to be the most effective sites that can play this role. This study may provide useful insights for design of new drugs to counter *E. coli* H7:O157 infection while avoiding cell wall modification, which may result in more aggressive strains of the bacterium.

The main limitation of this study is that it does not measure Shiga toxin production in the mutated bacterium. This measurement can confirm speculation of increased pathogenicity due to over-production of Shiga toxins.

Supplementary Materials: Data recorded, samples collected, questionnaires, and genomic DNA, and PCR products used during this study are available and stored at https://zenodo.org/uploads/14623186 with DOI: 10.5281/zenodo.14623186

Author Contributions: W.A.S. performed sample collection, DNA extraction, and PCR amplification; R.N.A. performed data analysis and article drafting; and I.A.A. supervised the progress of the project. All authors

have read and agreed to the published version of the manuscript.

Funding:

This research received no external funding.

Institutional Review Board Statement: This study was approved by the College of Veterinary Medicine IRB and animal welfare committee and was issued with approval no. PG/244.

Informed Consent Statement: All authors approved the publication of the article after reviewing the results, discussion, and draft.

Data Availability Statement: The data recorded, samples collected, questionnaires, genomic DNA, and PCR products used during this study are available and stored at https://zenodo.org/uploads/14623186 with DOI 10.5281/zenodo.14623186.

Conflicts of Interest: This research was conducted without any competing interests among the authors or any other research group at other institutions..

References

[1] Fontaine, R.; Arnon, S.; Martin, W. Raw hamburger: An interstate common source of human salmonellosis. Am. J. Epidemiol. 1978, 107, 36–45. https://doi.org/10.1093/oxfordjournals.aje.a112505.

[2] Ahmed, S.T.; Jasim, A.N.; Ali, A.M. Isolation and characterization E. coli O157:H7 from meat and cheese and detection of Stx1, Stx2, hlyA, eaeA using multiplex PCR. JOBRC 2011, 5, 15–24.

[3] Thompson, J.S.; Hodge, D.S.; Borczyk, A.A. Rapid biochemical test to identify verocytotoxin-positive strains of Escherichia coli serotype O157. J. Clin. Microbiol. 1990, 28, 2165–2168.

[4] Blanco, M.; Blanco, J.; Mora, A.; Dahbi, G.; Alonso, M.; González, E. Serotypes, virulence genes, and intimin types of Shiga toxin (verotoxin)-producing Escherichia coli isolates from cattle in Spain and identification of a new intimin variant gene (eae-xi). J. Clin. Microbiol. 2004, 42, 645–651.

[5] Al-Khyat, F. Enterohaemorrhagic E. coli O157 in locally produced soft cheese. Iraqi J. Vet. Med. 2008, 32, 88–99.

[6] Guth, B.; Prado, V.; Rivas, M. Shiga toxin-producing Escherichia coli. In Pathogenic Escherichia coli in Latin America, Torres, A.G., Ed.; Department of Microbiology and Immunology, Sealy Institute for Vaccine Sciences, University of Texas Medical Branch: Galveston, TX, USA, 2010.

[7] Paton, A.W.; Paton, J.C. Direct detection of Shiga toxigenic Escherichia coli strains belonging to serogroups O111, O157, and O113 by multiplex PCR. J. Clin. Microbiol. 1999, 37, 3362–3365.

[8] Heiman, K.E.; Mody, R.K.; Johnson, S.D.; Griffin, P.M.; Gould, L.H. Escherichia coli O157 outbreaks in the United States, 2003–2012. Emerg. Infect. Dis. 2015, 21, 1293–1301. https://doi.org/10.3201/eid2108.141364.

[9] Van, T.T.H.; Yidana, Z.; Smooker, P.M.; Coloe, P.J. Antibiotic use in food animals worldwide, with a focus on Africa: Pluses and minuses. J. Glob. Antimicrob. Resist. 2020, 20, 170–177. https://doi.org/10.1016/j.jgar.2019.07.031.

[10] Mohammed, Z.A. Isolation and Identification of Escherichia coli O157:H7 from locally minced meat and imported minced and chicken meat. Iraqi J. Vet. Med. 2008, 32, 100–113.

[11] Hasan, J.M.; Najim, S.S. A review of the Prevalence of Enterohemorrhagic E. coli in Iraq. JOBRC 2024, 18, 33–39.

[12] Khalil, Z.K. Isolation and identification of Staphylococcus aureus, Listeria monocytogenes, E. coli O157:H7 and Salmonella specious from raw beef and lamb meat in Baghdad by PCR. Iraqi J. Sci. 2016, 57, 1891–1897.

[13] Lim, J.M.; Singh, S.R.; Duong, M.C.; Legido-Quigley, H.; Hsu, L.Y.; Tam, C.C. Impact of national interventions to promote responsible antibiotic use: A systematic review. J. Antimicrob. Chemother. 2020, 75, 14–29. https://doi.org/10.1093/jac/dkz348.

[14] Nataro, J.P.; Kaper, J.B. Diarrheagenic Escherichia coli. Clin. Microbiol. Rev. 1998, 11,142–201. https:// 10.1128/cmr.11.1.142. Caprioli A, Morabito S, Brugere H, Oswald E. Enterohaemorrhagic Escherichia coli: Emerging issues on virulence and modes of transmission. Vet. Res. 2005, 36, 289–311. https://doi.org/10.1051/vetres:2005002.

[15] Beata, S.; Michał, T.; Mateusz, O.; et al. Norepinephrine affects the interaction of adherent-invasive Escherichia coli with intestinal epithelial cells. Virulence 2021, 12, 630–637. https://doi.org/10.1080/21505594.2021.1882780.

[16] Perna, N.T.; Plunkett, G.; Burland, V.; Mau, B.; Glasner, J.D.; Rose, D.J.; Mayhew, G.F.; Evans, P.S.; Gregor, J.; Kirkpatrick, H.A.; et al. Genome sequence of enterohaemorrhagic Escherichia coli O157:H7. Nature 2001, 409, 529–533.

[17] Dobrindt, U.; Agerer, F.; Michaelis, K.; Janka, A.; Buchrieser, C.; Samuelson, M.; Svanborg, C.; Gottschalk, G.; Karch, H.; Hacker, J. Analysis of genome plasticity in pathogenic and commensal Escherichia coli isolates by use of DNA arrays. J. Bacteriol. 2003, 185, 1831–1840.

[18] Wick, L.M.; Qi, W.; Lacher, D.W.; Whittam, T.S. Evolution of genomic content in the stepwise emergence of Escherichia coli O157:H7. J. Bacteriol. 2005, 187, 1783–1791.

[19] Amézquita-López, B.A.; Quiñones, B.; Soto-Beltrán, M.; et al. Antimicrobial resistance profiles of Shiga toxin-producing Escherichia coli O157 and non-O157 recovered from domestic farm animals in rural communities in Northwestern Mexico. Antimicrob. Resist. Infect. Control. 2016, 5, 1. https://doi.org/10.1186/s13756-015-0100-5.

[20] Aklilu, F.; Daniel, K.; Ashenaf, K. Prevalence and antibiogram of Escherichia coli O157 isolated from bovine in Jimma, Ethiopia: Abattoir-based survey. Ethiop. Vet. J. 2017, 21, 109–120.

[21] Tarekegn, A.A.; Mitiku, B.A.; Alemu, Y.F. Escherichia coli O157:H7 beef carcass contamination and its antibiotic resistance in Awi Zone, Northwest Ethiopia. Food Sci. Nutr. 2023, 11, 6140–6150.

[22] Gambushe, S.M.; Zishiri, O.T.; E El Zowalaty, M. Review of Escherichia coli O157:H7 Prevalence, Pathogenicity, Heavy Metal and Antimicrobial Resistance, African Perspective. Infect. Drug Resist. 2022, 15, 4645–4673.

[23] Banerjee, S.; Lo, K.; Ojkic, N.; Stephens, R.; Scherer, N.F.; Dinner, A.R. Mechanical feedback promotes bacterial adaptation to antibiotics. Nat. Phys. 2021, 17, 403–409.

[24] Harris, L.K.; Theriot, J.A. Relative rates of surface and volume synthesis set bacterial cell size. Cell 2016, 165, 1479–1492.

[25] Assefa, A.; Garcias, B.; Mourkas, E.; Molina-López, R.; Darwich, L. Global distribution of antimicrobial resistance genes in Escherichia coli isolated from wild animals using genomes available in public databases. Sci. Total Environ. 2025, 985, 179742.

[26] Ojkic, N.; Banerjee, S. Bacterial cell shape control by nutrient-dependent synthesis of cell division inhibitors. Biophys. J. 2021, 120, 2079–2084.

[27] Ojkica, N.; Serbanescua, D.; Banerjee, S. Antibiotic Resistance via Bacterial Cell Shape-Shifting. mBio 2022, 13, e0065922. https://doi.org/10.1128/mbio.00659-22.

[28] Nikolic, P. and Mudgil P. The Cell Wall, Cell Membrane and Virulence Factors of Staphylococcus aureus and Their Role in Antibiotic Resistance. Microorganisms 2023, 11, 259. https://doi.org/10.3390/microorganisms11020259.

[29] WHO. WHO Estimates of the Global Burden of Foodborne Diseases: Foodborne Disease Burden Epidemiology Reference Group 2007–2015; WHO: Geneva, Switzerland, 2016.

[30] March, S.B.; Ratnam, S. Sorbitol-MacConkey Medium for Detection of Escherichia coli 0157:H7 Associated with Hemorrhagic Colitis. J. Clin. Microbiol. 1986, 23, 869–872.

[31] Leininger, D.J.; Roberson, J.R.; Elvinger, F. Use of eosin methylene blue agar to differentiate Escherichia coli from other gram-negative mastitis pathogens. J. Vet. Diagn. Invest. 2001, 13, 273–275.

[32] Ally, C. Antony, Mini K. Paul, Reshma Silvester, Aneesa P.A., Suresh K., Divya P.S., Simmy Paul, Fathima P.A. and Mohamed Hatha Abdulla. Comparative Evaluation of EMB Agar and Hicrome E. coli Agar for Differentiation of Green Metallic Sheen Producing Non-E. coli and Typical E. coli Colonies from Food and Environmental Samples. J. Pure Appl. Microbiol. 2016, 10, 2863–2870.

[33] Rani, A.; Ravindran, V.B.; Surapaneni, A.; Mantri, N.; Ball, A.S. Review: Trends in point-of-care diagnosis for Escherichia coli O157:H7 in food and water. Int. J. Food Microbiol. 2021, 349, 109233.

[34] Pagnout, C.; Sohm, B.; Razafitianamaharavo, A.; Caillet, C.; Offroy, M.; Leduc, M.; Gendre, H.; Jomini, S.; Beaussart, A.; Bauda, P.; et al. Pleiotropic effects of rfa-gene mutations on Escherichia coli envelope properties. Sci. Rep. 2019, 9, 9696. https://doi.org/10.1038/s41598-019-46100-3.

[35] Raetz, C.R.; Whitfield, C. Lipopolysaccharide endotoxins. Annu. Rev. Biochem. 2002, 71, 635–700.

[36] Han, W.; Wu, B.; Li, L.; Zhao, G.; Woodward, R.; Pettit, N.; Cai, L.; Thon, V.; Wang, P. Defining Function of Lipopolysaccharide O-antigen Ligase WaaL Using Chemoenzymatically Synthesized Substrates. Microbiology 2012, 287, 5357–5365.

[37] Abeyrathne, P.D.; Daniels, C.; Poon, K.K.H.; Matewish, M.J.; Lam, J.S. Functional Characterization of WaaL, a Ligase Associated with Linking O-Antigen Polysaccharide to the Core of Pseudomonas aeruginosa Lipopolysaccharide. J. Bacteriol. 2005, 187, 3002–3012. https://doi.org/10.1128/JB.187.9.3002-3012.2005.

[38] Klena, J.D.; Ashford, R.S., II; Schnaitman, C.A. Role of Escherichia coli K-12 rfa genes and the rfp gene of Shigella dysenteriae 1 in generation of lipopolysaccharide core heterogeneity and attachment of O antigen. J. Bacteriol. 1992, 174, 7297–7307. doi.org/10.1128/jb.174.22.7297-7307.1992

[39] Kaniuk, N.A.; Monteiro, M.A.; Parker, C.T.; Whitfield, C. Molecular diversity of the genetic loci responsible for lipopolysaccharide core oligosaccharide assembly within the genus Salmonella. Mol. Microbiol. 2002, 46, 1305–1318.

[40] Frirdich, E.; Lindner, B.; Holst, O.; Whitfield, C. Overexpression of the waaZ Gene Leads to Modification of the Structure of the Inner Core Region of Escherichia coli Lipopolysaccharide, Truncation of the Outer Core, and Reduction of the Amount of O Polysaccharide on the Cell Surface. J. Bacteriol. 2003, 185, 1659–1671. https://doi.org/10.1128/JB.185.5.1659-1671.2003.

[41] Yethon, J.A.; Heinrichs, D.; Monteiro, M.A.; Perry, M.B.; Whitfield, C. Involvement of waaY, waaQ, and waaP in the Modification of Escherichia coli Lipopolysaccharide and Their Role in the Formation of a Stable Outer Membrane. J. Biol. Chem. 1998, 273, 26310–26316.

[42] Taylor, C.M.; Goldrick, M.; Lord, L.; Roberts, I.S. Mutations in the waaR Gene of Escherichia coli Which Disrupt Lipopolysaccharide Outer Core Biosynthesis Affect Cell Surface Retention of Group 2 Capsular Polysaccharides. J. Bacteriol. 2006, 188, 1165–1168. https://doi.org/10.1128/JB.188.3.1165-1168.2006.

[43] Al wendawi, S.H.A.; Al Rekaby, S.M. The Effeciency of Enteric Lactobacillus in Preventing Hemorrhagic Colitis and

Blocking Shiga Toxins Productions in Rats Models Infected with Enterohemorrhagic Escherichia coli (EHEC). Iraqi J. Agric. Sci. 2021, 52, 1346–1355.

[44] Al-Taii, D.H.F. Effects of E. coli O157:H7 Experimental Infections on Rabbits. Iraqi J. Vet. Med. 2019, 43, 34–42.

[45] Wang, J.; Ma, W.; Wang, X. Insights into the structure of Escherichia coli outer membrane as the target for engineering microbial cell factories. Microb. Cell Fact. 2021, 20, 73. https://doi.org/10.1186/s12934–021–01565–8.

[46] Kaper, J.B.; Nataro, J.P.; Mobley, H.L. Pathogenic Escherichia coli. Nat. Rev. Microbiol. 2004, 2, 123–140.

[47] Croxen, M.A.; Finlay, B.B. Molecular mechanisms of Escherichia coli pathogenicity. Nat. Rev. Microbiol. 2010, 8, 26–38.

[48] Sora, V.M.; Meroni, G.; Martino, P.A.; Soggiu, A.; Bonizzi, L.; Zecconi, A. Extraintestinal Pathogenic Escherichia coli: Virulence Factors and Antibiotic Resistance. Pathogens 2021, 10, 1355, https://doi.org/10.3390/pathogens10111355.

[49] Khaleq, M.A.A.; Abd, A.H.; Dhahi, M.A. Efficacy of Combination of Meropenem with Gentamicin, and Amikacin against Resistant E. coli Isolated from Patients with UTIs: In vitro Study. Iraqi J. Pharm. Sci. 2011, 20, 66–74.

[50] Khan Md, F.; Rashid, S.S. Molecular Characterization of Plasmid-Mediated Non-O157 Verotoxigenic Escherichia coli Isolated from Infants and Children with Diarrhea. Baghdad Sci. J. 2020, 17, 710–719.

[51] Wang, X.; Yu, D.; Chui, L.; Zhou, T.; Feng, Y.; Cao, Y.; Zhi, S. A Comprehensive Review on Shiga Toxin Subtypes and Their Niche-Related Distribution Characteristics in Shiga-Toxin-Producing E. coli and Other Bacterial Hosts. Microorganisms 2024, 12, 687. https://doi.org/10.3390/microorganisms12040687.

[52] O'Neil, J. Review on Antimicrobial Resistance Antimicrobial Resistance: Tackling a Crisis for the Healthand Wealth of Nations. Available online: https://amr-review.org/sites/default/files/AMR%20Review%20Paper%20-%20Tackling%20a%20crisis%20for%20the%20health%20and%20wealth%20of%20nations_1.pdf (accessed on 7 2023).

[53] Gray, D.A.; Wenzel, M. Multitarget approaches against multiresistant superbugs. ACS Infect. Dis. 2020, 6, 1346–1365. https://doi.org/10.1021/acsinfecdis.0c00001.

[54] Zhao, M.; Li, Y.; Wang, Z. Mercury and mercury-containing preparations: History of use, clinical applications, pharmacology, toxicology, and pharmacokinetics in traditional Chinese medicine. Front. Pharmacol. 2022, 13, 807807. https://doi.org/10.3389/fphar.2022.807807.

[55] Lekhan, A.; Turner, R.J. Exploring antimicrobial interactions between metal ions and quaternary ammonium compounds toward synergistic metalloantimicrobial formulations. Antimicrob. Chemother. 2024, 12, e0104724. https://doi.org/10.1128/spectrum.01047-24.